Geofísica Internacional (2004), Vol. 43, Num. 1, pp. 89-95

Numerical simulation of the cooling of a solar flare

César A. Mendoza-Briceño[1], Leonardo Sigalotti[2] and Neyda Y. Añez-Parra[1,3]
[1] *Centro de Astrofísica Teórica, Universidad de los Andes, Mérida, Venezuela*
[2] *Centro de Física, Instituto Venezolano de Investigaciones Científicas, IVIC, Caracas, Venezuela*
[3] *Departamento de Física, FEC, Universidad del Zulia, Maracaibo, Venezuela*

Received: March 31, 2002; accepted: September 17, 2002

RESUMEN

Se usa un código hidrodinámico unidimensional para estudiar el enfriamiento de destellos solares. El enfriamiento del flujo a través del tubo magnético se calcula para el caso en el cual la atmósfera se encuentra inicialmente en equilibrio térmico con una temperatura máxima de 10^7 K. A medida que el sistema se enfría, la evolución de la densidad, velocidad y temperatura se calcula como función de la altitud para diferentes longitudes del lazo. En este trabajo se usa la función de enfriamiento propuesta por Hildner (1974) modificada para incluir temperaturas por debajo de 10^4 K y el efecto de frenado para valores mayores de 10^6 K. Se encuentra que el tiempo de enfriamiento aumenta al aumentar la longitud del lazo. Por otro lado, si se considera una fuente de energía con variación espacial a lo largo del lazo, el tiempo de enfriamiento varía en comparación con el caso en el cual no hay calentamiento externo. En particular, se observa que éste disminuye a medida que la fuente se concentra siempre más en la base del lazo.

PALABRAS CLAVES: Destello solar, atmósfera solar, hidrodinámica.

ABSTRACT

A one-dimensional hydrodynamics code is used to study the cooling of solar flares. The cooling of the flux tube is calculated for the case in which the atmosphere is initially in thermal equilibrium with a maximum temperature of about 10^7 K. As the system cools, the evolution of the temperature, density, and velocity is calculated as a function of height for different lengths of the loop. We use the cooling function proposed by Hildner (1974), extended to include temperatures lower than 10^4 K and the Bremsstrahlung effect for values higher than 10^6 K. It is found that the cooling time increases as the length of the loop is increased. Furthermore, if a spatially-varying energy source is allowed along the loop length, the cooling time differs from the case with no external heating. In particular, it is seen to decrease as the input heating concentrates at the base of the loop.

KEY WORDS: Solar flare, Sun atmosphere, hydrodynamics.

1. INTRODUCTION

Investigation of the structure and dynamics of the solar atmosphere, specifically the upper hottest and magnetically dominated part of the solar corona, is an important and interesting branch of modern astrophysics. Despite significant progress in solar physics over several decades, a number of fundamental questions, e. g. concerning the physical mechanisms responsible for coronal heating, solar wind acceleration, and solar flares, still remain to be answered. The solution to these problems is of fundamental importance to progress in the fields of solar physics, stellar and magnetospheric physics, and laboratory plasma physics, and is needed to improve our current understanding of solar-terrestrial connections.

Observations from SOHO and TRACE are reviving interest on studying the dynamics of coronal loops by means of numerical simulations. Such models have been used to study large dynamical events like solar flares. Nagai (1980) proposed a dynamical model for the formation of soft X-ray emitting hot loops in solar flares. He considered a solar model atmosphere in a magnetic loop that changes its state and forms a hot loop when the flare energy is released in the form of heat at the top or around the transition region in the loop. Antiochos and Krall (1979) calculated the cooling process from the sudden disappearance of the energy source at the maximum phase of the solar flare; they found that the cooling time was too short to match the observations. Doschek *et al*. (1982) extended the work of Antiochos and Krall (1979) by including the upper chromosphere in their calculations, and they obtained cooling times of about 232 seconds. MacNeice (1986) studied numerically the thermal development of a heated coronal loop by a transient heating pulse centred about the loop apex. He showed that it was difficult to perform calculations continuously from the impulsive to the gradual phase. A simple method to investigate the cooling mechanisms of flare loops at different temperatures, den-

sities and loop lengths was proposed by Svetska (1987). Gan and Fang (1990) studied the gradual phase of a solar flare with improvements in the radiative loss function, the resolution on the transition region, and the energy deposition in the chromosphere by the coronal soft X-ray emission. More recently, Schmieder *et al*. (1996a, 1996b) employed similar models to those of Svestka (1987) by also improving the radiation loss function. They found longer cooling times and applied their results to the post-flare loops of 26 June 1992. Cargill *et al*. (1995) reexamined the existing theoretical models of the cooling of flare plasma by assuming that the cooling occurs in two separate phases, with one phase being dominated by conduction and the other by radiation, and derived a simple analytic expression for the cooling time of the flare. In this paper, we perform hydrodynamical simulations of the evolution of a solar flare plasma from the maximum of the gradual phase. In section 2 we write down the basic equations and describe the boundary conditions used to solve them. In section 3 we discuss the main results of our loop model calculations and in section 4 we summarize the relevant conclusions.

2. BASIC EQUATIONS

The magnetic field plays an important role in the solar corona, producing in it a complex network of individual loop-like structures. The coronal plasma β is much smaller than unity (with typical values of $\sim 10^{-2}$) and the velocities are less than the Alfvén speed. Therefore, it can be assumed that a strong magnetic field confines the plasma in such a way as to provide a symmetric loop geometry that channels both the mass flow and the heat flux. Thus, in a first approximation motion of the plasma along the confining magnetic field can be described by solving the governing equations in one-space dimension. One-dimensional (1D) fluid models are physically justified because the corona and transition region are typically at a low β. Under this condition, the plasma dynamics is dominated by the magnetic field and so the plasma macroscopic motion takes place primarily along the magnetic field lines. In addition, thermal conduction, due to the electron diffusion, also occurs along the field lines rather than across them (Spitzer, 1962). In this way, each plasma loop can be treated almost independently from the neighboring ones (Rosner *et al*., 1978), implying that the thermo-dynamical evolution of the coronal plasma along the field lines is essentially 1D. It is also worth to mention that for most loops made of magnetically confined plasma the Alfvén travel time $t_A = L/v_A$ (where L is the characteristic field line length and $v_A = B/\sqrt{4\pi\rho}$ the Alfvén speed, with B the magnetic induction and ρ the plasma mass density) is much shorter than the plasma evolution time, implying that in most loops the magnetic field structure does not change appreciably during the plasma evolution. Thus, unless changes in the magnetic field occur within a few Alfvén times, each loop behaves as a rigid pipe filled with coronal plasma.

The scope of loop modelling is rather broad and one may foresee many new developments that will demand the use of more advanced numerical techniques and the allowance for two- and three-space dimensions. While 1D models involve less computational burden and may describe qualitatively well the main features of the thermo-dynamical evolution of most loops, they are not able to account for the plasma-magnetic field interaction that could occur in some other real loops. For instance, TRACE observations have clearly shown that loops are composed of many filaments with a cross-field structure, which, in some cases, may evolve differently. This will demand studying the evolution of multi-loop models through the use of magnetohydrodynamics (MHD) codes in two and three dimensions.

Defining the spatial variable s as the position along a loop of constant cross-sectional area, the mass, momentum, and energy conservation equations in one-space dimension, including radiative cooling and heating, thermal conduction, and gravity, reduce to

$$\frac{\partial \rho}{\partial t} + \frac{\partial (\rho v)}{\partial s} = 0, \tag{1}$$

$$\frac{\partial (\rho v)}{\partial t} + \frac{\partial (\rho v^2)}{\partial s} = -\frac{\partial p}{\partial s} - \rho g_{\parallel}(s), \tag{2}$$

$$\frac{\partial (\rho T)}{\partial t} + \frac{\partial (\rho v T)}{\partial s} = -\frac{\mu(\gamma - 1)}{R_g} \left[p \frac{\partial v}{\partial s} + \mathcal{L}(\rho, T, s) - \frac{\partial}{\partial s}\left(\kappa \frac{\partial T}{\partial s} \right) \right], \tag{3}$$

where ρ is the (mass) density, v is the fluid velocity along a fixed magnetic field line, T is the temperature, p is the gas pressure, γ (=5/3) is the ratio of specific heats and $\kappa = \kappa_{\parallel} \approx 10^{-11}\, T^{5/2}\ \mathrm{Wm^{-1}\,K^{-1}}$ is the coefficient of thermal conductivity parallel to the magnetic field (Braginskii, 1965). Equations (1)-(3) can be solved in closed form for given initial and boundary conditions once a constitutive relation for the pressure is specified. Here we assume an equation of state (EOS) of the form

$$p = \frac{R_g}{\mu} \rho T, \tag{4}$$

where μ denotes the mean molecular weight.

The gravitational acceleration $g_{\parallel}(s)$ is assumed to depend only on position along the loop and is given by

$$g_{\parallel}(s) = -g_{solar} \cos\left[\frac{\pi}{2} \frac{(L - s)}{L} \right] = -g_{solar} \sin\left(\frac{\pi s}{2L} \right), \tag{5}$$

where $g_{solar} = 2.7 \times 10^4$ cm s^{-2} is the solar gravity. This form specifies the component of the gravitational force along a magnetic field line of semi-circular shape only (see Figure 1). At the summit $s = 0$, $g_{\parallel}(0)=0$, while at the footpoint $s = L$, $g_{\parallel}(L) = -g_{solar}$.

The radiative loss-gain function $\mathcal{L}$ on the right-hand side of Equation (3) is in general given by the expression

$$\mathcal{L}(\rho,T,s) = \rho^2 Q(T) - H(s,t), \tag{6}$$

where $Q(T)$ is the optically thin energy loss function and $H(s,t)$ is the unknown coronal heating term. For the present models, $Q(T)$ is approximated by a piecewise continuous function of the form

$$Q(T) = \chi T^{\alpha}, \tag{7}$$

where χ and α are radiative loss coefficients (Hildner, 1974; Rosner *et al.*, 1978), which take constant values within any particular range of temperature of the piecewise fitting. Furthermore, since the mechanism of coronal heating is not known, the heating function is assumed to have the form

$$H(s,t) = H(s) = h_0 \exp\left[-\frac{(L-s)}{s_H}\right] \tag{8}$$

for $0 \le s \le L$ (Rosner *et al.*, 1978). Here h_0 is the heating deposition at the base ($s = L$) of the loop, s_H is the spatial decay-length of the heating source, and L is half the length of the loop measured from $s = 0$ (at the top) to $s = L$ (at the base). This form of the heating mechanism represents waves that are damped in the corona so that the amount of energy supplied to the loop will decay from the base towards the summit over some spatial scale small compared to the loop length and specified by the parameter s_H.

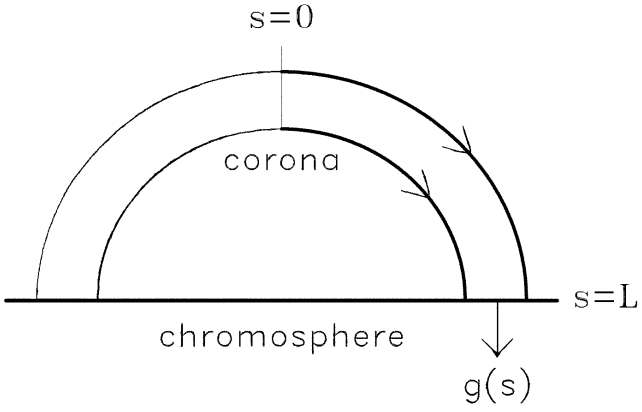

Fig. 1. Geometry of the semi-circular loop model. Reflection symmetry is applied at the summit ($s = 0$) so that only half of the loop is represented by the calculations. Boundary conditions are specified at the base ($s = L$) of the loop by fixing the density and temperature there.

The heating – which maintains the coronal plasma at temperatures of the order of million degrees and whose variation may be responsible for many of the observed changes – is a fundamental component of any coronal model and its formulation may depend on the specific problem. It is beyond any doubt that the coronal magnetic field coupled with turbulent motions of the photosphere plays a crucial role in the coronal heating. However, the question arises of whether this magnetic energy is dissipated by MHD waves propagating through the solar atmosphere or by small scale magnetic reconnection sites throughout the coronal magnetic network. Also, it has been recognized that the heat input to the corona is likely to be episodic (e.g., dynamic or time dependent).

To date, two broad-range possibilities for the heating mechanism have been studied: direct current (DC) dissipation and alternating current (AC) dissipation. This division is based on the timescale of response of the solar corona to the motions of the underlying photosphere (Zirker, 1993). The driving timescale can either be assumed to be longer than the Alfvén transit time across a coronal structure (DC) or shorter (AC). If the deformations of the magnetic field have timescales comparable to, or shorter than, the time required for an Alfvén wave to traverse a coronal loop, then the field behavior is described in terms of waves. The turbulent motions in the convective zones launch waves that propagate through the chromosphere and into the corona. Under proper conditions, these waves can then deposit part of their energy into the surrounding chromospheric or coronal plasma (Ulmschneider, 1996). Other kinds of waves that could be responsible for the heating are slow mode MHD waves and longitudinal MHD tube waves with dissipation mechanisms by shock; fast mode MHD waves dissipated by Landau damping; Alfvén waves (transverse and torsional) dissipated by mode-coupling, resonance heating, and compressional viscous heating; and magnetoacoustic surface waves dissipated by mode coupling, phase mixing, and resonant absorption. While none of these mechanisms can by itself explain the total heating, each of them could play an important role in a particular specific region.

The set of Equations (1)-(4), together with the definitions (5)-(8), can be solved for given initial and boundary conditions. The initial conditions are specified by setting the density, velocity, and temperature profiles at $t = 0$, i.e.,

$$\rho_i = \rho(s,0);\ v_i = v(s,0);\ T_i = T(s,0), \tag{9}$$

with $v(s,0)$ usually taken to be zero. In all cases, the boundary conditions are defined by specifying the density and tem-

perature at the base of the loop. In particular, we choose constant values of ρ and T at $s = L$, that is

$$T(L,t) = T_b\,;\;\; \rho(L,t) = \rho_b\,, \qquad (10)$$

for $t \geq 0$. Given the EOS (4), this is equivalent to set a constant-pressure boundary condition at the footpoint. Here we restrict ourselves to study only symmetrical loops in which the location of the summit is held fixed in space and time. As shown in Figure 1, at $s = 0$ we set reflective boundary conditions by setting the velocity and all gradients to zero. In this way, the density and temperature at the summit are evolved hydrodynamically while keeping their spatial derivatives exactly vanishing there. Also, in order to mimic the presence of a deep chromosphere, mass is allowed to flow across the loop base ($s = L$) by just evolving the fluid velocity there.

We solve Equations (1)-(4) using a one-dimensional, finite-difference hydrodynamics code based on a modified version of the second-order accurate, Lagrangian-remap technique introduced by Lufkin and Hawley (1993). The source terms in the momentum and internal energy equations are advanced in time through a multistep solution procedure, in which each contribution is evaluated separately. For each substep, the temporal integration is made either explicitly or implicitly depending on the timestep restrictions for stability, and is made second-order accurate by means of a predictor-corrector approach. The Lagrangian solution is then remapped onto an Eulerian grid, which can be either fixed or moving. The remap procedure is based on a conservation-law form of the hydrodynamic equations and advection is performed using the van Leer (1977) monotonic interpolation scheme. A more detailed account of the code and tests that have been made to validate its accuracy can be found in Sigalotti and Mendoza-Briceño (2003).

3. RESULTS

3.1 The effects of varying the length of the loop

In this section, we consider the effects of varying the length of the loop on the cooling time of the flare for five loop model calculations with increasing length.

In Figure 2, we show the temperature at the top of the loop as a function of time for all models considered. In all cases, the initial equilibrium is left to evolve starting with a temperature profile with maximum temperature of 10^7 K at the summit and $h_0 = 0$ in Equation (8) so that there is no input of energy. All models behave in a qualitatively similar manner. Based on the temperature plots of Figure 2, the evolution can be subdivided into four main stages. The first stage is characterized by a short period in which the top regions cool down rapidly, due to the effects of thermal conduction, while approximately maintaining a constant density. As a result, the coronal plasma just away from the top region is mainly heated by thermal conduction. This stage lasts until a small bump occurs in the temperature around $T \sim 3.2 \times 10^6$ K. For temperatures higher than this, the characteristic cooling time by conduction is shorter than that by radiative losses (see section 4). By the end of this stage, a bump in the top temperature is produced as the slightly hotter plasma away from the top flows toward it causing a sudden slight increase of the temperature. Balance of energy is rapidly established and thereafter the top cools down smoothly. During this second stage of the evolution, cooling by radiative losses is partially balanced by heating due to mechanical transport of hotter material toward the top region, causing it to cool gradually until temperatures of about 6 x 10^5 K are reached. At these values, cooling by thermal conduction does no longer contribute to counterbalance heating by mechanical transport and therefore the top temperature slightly increases leading to a second bump. A third stage begins when the characteristic cooling time by radiative losses becomes much shorter than the other timescales (see section 4, Figure 4), leading to a rapid decrease of the temperature. As shown in Figure 2, the temperature drops by almost two orders of magnitude in a few seconds after which the plasma evolves to a new equilibrium at chromospheric values. Thereafter, the temperature keeps constant for the remainder of the evolution (fourth stage).

As long as the total length of the loop is increased, the cooling time (first and second stages) increases, with the top

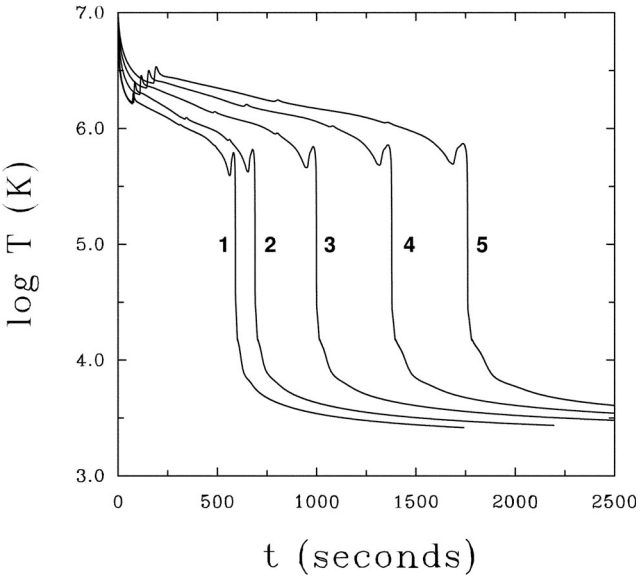

Fig. 2. Time variation of the summit temperature showing the cooling of five solar flare models with loop lengths: 4.0 x 10^9 cm (curve 1), 5.5 x 10^9 cm (curve 2), 8.0 x 10^9 cm (curve 3), 1.1 x 10^{10} cm (curve 4), and 1.4 x 10^{10} cm (curve 5). For all models, the evolution has been obtained setting $h_0 = 0$ in Equation (8) (case with no input heating).

region achieving slightly lower temperatures in loops of shorter length. This is easily understandable because the counterbalancing effects of heating due to mechanical transport takes longer in loops of increasing length. In particular, when the length of the loop is of the order of 4 x 10^9 cm, the flare cools down in about 1700 s, whereas for a length of the order of 1.4 x 10^{10} cm the cooling time increases to about 3000 s. We note that the cooling time also depends on whether the operating cooling mechanism is conductive or radiative. At high temperatures (~10^6 K), the energy is mainly dissipated by thermal conduction. On the contrary, when the plasma reaches lower values of the temperature, the dominant mechanism is the loss of energy by radiation.

3.2 The effects of heating

In this section, we describe the hydrodynamical evolution of five more loop models using the heating function as given by Equation (8), with $h_0 = 10^{-3}$ erg cm^{-3} s^{-1}. All models start from equilibrium conditions, sharing the same length ($L = 1.4 \times 10^{10}$ cm) and differing only in the spatial energy distribution through the decay length of the heating s_H. In particular, we consider values of $s_H / L = 0.01$, 0.05, 0.1, 0.5 and 10^{81}. A value as high as 10^{81} is used to mimic a uniform heating ($s_H \rightarrow \infty$) along the loop. On the other hand, a value as low as 0.01 represents models in which the heating is more concentrated at the base of the loop.

The results of the evolutions in terms of the time variation of the top temperature are displayed in Figure 3. Those models starting with a more localized heating source (i.e., $0.01 \leq s_H / L \leq 0.1$) behave quite similarly as shown by curves 1-3 of Figure 3. The time dependence of the top temperature as well as the cooling time resulting for these three models are also quite similar to those of the longest loop shown in Figure 2 (curve 5) for the case of no input energy. As the heating source becomes less localized ($s_H / L = 0.5$, curve 4) or even uniformly distributed along the loop ($s_H \rightarrow \infty$, curve 5) more heating is allowed into the system and as a consequence the plasma cools down considerably more slowly than in cases where the heating is negligible. This is clearly seen in Figure 3, where after the first bump in the temperature variation, the top region evolves in close thermal equilibrium for more than 2000 s (curve 4) and 3000 s (curve 5). Thereafter, catastrophic cooling occurs in both cases as cooling due to radiative losses dominates the evolution, causing the coronal plasma to reach chromospheric temperatures in a few seconds.

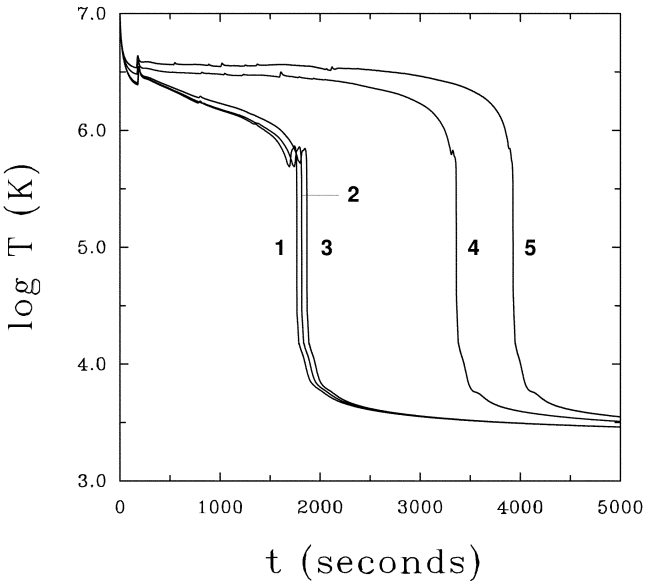

Fig. 3: Time variation of the summit temperature showing the cooling of five solar flare models of length 1.4 x 10^{10} cm as obtained using the heating function given by Equation (8) with $h_0 = 10^{-3}$ erg cm^{-3} s^{-1} and varied values of the decay length of the heating: (curve 1), 0.05 (curve 2), 0.1 (curve 3), 0.5 (curve 4), and ∞ (curve 5).

The results indicate that the cooling time increases from less than 2000 s, when the heating is negligible, to more than 4000 s, when the value of s_H / L is high enough that the heating can be considered to be uniform along the loop. As expected, compared with the no heating case (curve 5 of Figure 2), the cooling time also increases when the heating is more or less distributed along the loop length.

4. DISCUSSION

In this paper we have used numerical simulations to investigate the cooling time for the gradual phase of a solar flare, starting from equilibrium initial conditions. The effects of varying the length of the loop on the cooling time were first considered. The results imply that the cooling time increases as long as the length of the loop is increased. During this process, the coronal part cools mainly by thermal conduction, while the chromospheric part does it by radiative losses. This can be easily assessed by estimating both the radiation and conductive characteristic cooling times directly from Equation (3). Under the assumption that one mechanism dominates over all other processes, we obtain the following expressions

$$\tau_{\rm rad} = \frac{p}{(\gamma - 1)\rho^2 \chi T^{\alpha}}, \qquad (11)$$

and

$$\tau_{\rm cond} = \frac{pL^2}{(\gamma - 1)\kappa T^{1/2}}, \qquad (12)$$

for the radiation and conductive timescales, respectively. The variation of these timescales with temperature is shown in Figure 4 for the loop model evolution shown in Figure 2 (curve 4), with length $L = 1.1$ x 10^{10} cm. We see that at tem-

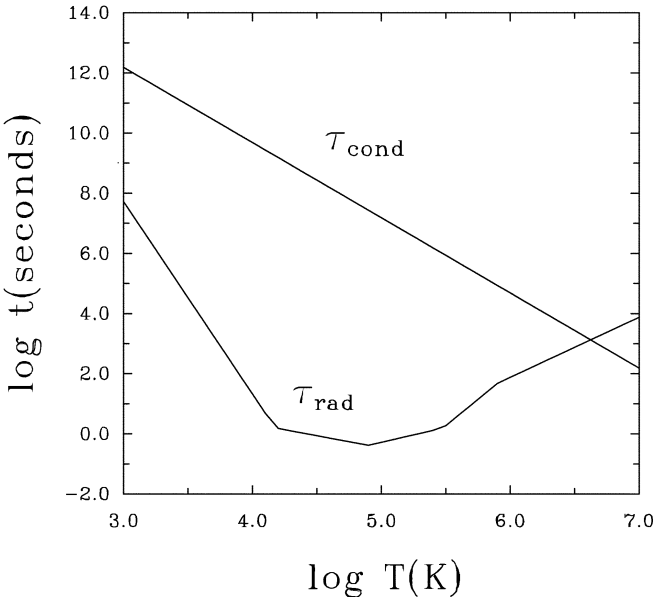

Fig. 4. Radiative (τ_{rad}) and conductive (τ_{cond}) characteristic cooling times as functions of the temperature. Both curves are obtained using Equations (11) and (12) for the flare evolution model corresponding to curve 4 of Figure 2. Similar plots are obtained for all other models considered.

peratures $T > 3.9 \times 10^6$ K, thermal conduction is the dominating cooling mechanism, while for lower temperatures energy losses by radiation dominates over conduction. In particular, in the range of temperatures between 1.0×10^4 and 5.0×10^5 K, the radiation cooling time becomes shorter than about 100 s, reaching a minimum value of ≈0.4 s when $T \approx 7.9 \times 10^4$ K. This explains the catastrophic cooling to chromospheric values seen in Figures 2 and 3. Similar curves to those shown in Figure 4 are also obtained for all other evolutions displayed in Figure 2.

When an energy input is included the cooling time becomes longer as more heating goes into the system. While for these calculations we have used a coronal heating function that depends only on the spatial variable, it is important to remark that excluding the heating in model calculations of the cooling of solar flares can lead to a mis-interpretation of the observations. For instance, flares are also observed in other stars and information about their length comes primarily from their estimated cooling time. In this respect, one important implication of the present results is that the cooling time can also be affected by the heating. So more work is needed in this direction perhaps using different forms of the heating in order to discern more precisely how the energy input may affect the cooling time.

ACKNOWLEDGEMENTS

We thank the referees for providing a number of valuable suggestions and comments that have improved both the style and content of the manuscript. One of us (C. A. M-B.) would like to thank the CDCHT of the Universidad de los Andes for financial support.

BIBLIOGRAPHY

ANTIOCHOS, S. K. and K. R. KRALL, 1979. The Evolution of Soft X-Ray-Emitting Flare Loops. *Astrophys. J., 229,* 788.

BRAGINSKII, S. I., 1965. Transport Processes in a Plasma. *Rev. Plasma Phys., 1,* 205.

CARGILL, P. J., J. T. MARISKA and S. K. ANTIOCHOS, 1995. Cooling of Solar Flare Plasmas. I. Theoretical Considerations. *Astrophys. J., 439,* 1034.

DOSCHEK, G. A., J. P. BORIS, C. C. CHENG, J. T. MARISKA and E. S. ORAN, 1982. A Numerical Simulation of Cooling Coronal Flare Plasma. *Astrophys. J., 258,* 373.

GAN, W. Q. and C. FANG, 1990. A Hydrodynamic Model of the Gradual Phase of the Solar Flare Loops. *Astrophys. J., 358,* 328.

HILDNER, E., 1974. The Formation of Solar Quiescent Prominences by Condensation. *Solar Phys., 35,* 23.

LUFKIN, E. A. and J. F. HAWLEY, 1993. The Piecewise-Linear Predictor-Corrector Code: A Lagrangian-Remap Method for Astrophysical Flows. *Astrophys. J. S., 88,* 569.

MACNEICE, P., 1986. A Numerical Hydrodynamic Model of Heated Coronal Loop. *Solar Phys., 103,* 47.

NAGAI, F., 1980. A Model of Hot Loops Associated with Solar Flares. I. Gas Dynamics in the Loop. *Solar Phys., 68,* 357.

ROSNER, R., W. H. TUCKER and G. S. VAIANA, 1978. Dynamics of the Quiescent Solar Corona. *Astrophys. J., 220,* 643.

SIGALOTTI, L. DI G. and C. MENDOZA-BRICEÑO, 2003. Dynamics of Solar Coronal Loops. *Astron. Astrophys., 397,* 1083.

SCHMIEDER, B., P. HEINZEL, L. VAN DRIEL-GESZTELYI and J. R. LEMEN, 1996a. Post-Flare Loops of 26 June 1992. *Solar Phys. 165,* 303.

SCHMIEDER, B., P. HEINZEL, J. E. WIIK, J. LEMEN, B. ANWAR, P. KOTRC and E. HIEI, 1996b. Relation between Cool and Hot Post-Flare Loops of 26 June 1992 Derived from Optical and X-Ray (SXT-YOHKOH) Observations. *Solar Phys., 156,* 337.

SPITZER, L., 1962. Physics of Fully Ionized Gases, Interscience Publishers, New York.

SVESTKA, Z., 1987. Cooling of Coronal Flare Loop through Radiation and Conduction. *Solar Phys., 108,* 411.

ULMSCHNEIDER, P., 1996. Chromospheric and Coronal Heating Mechanisms. *In:* Cool Stars, Stellar Systems and the Sun, eds. R. Pallavicini and A. K. Dupree, Astr. Soc. Pacific Conf. Series, *109,* 71.

VAN LEER, B., 1977. Towards the Ultimate Conservative Difference Scheme. V. A Second-Order Sequel to Godunov's Method. *J. Comput. Phys., 32,* 101.

ZIRKER, J., 1993. Coronal Heating. *Solar Phys., 148,* 43.

César A. Mendoza-Briceño[1], Leonardo Sigalotti[2] and Neyda Y. Añez-Parra[1,3]

[1] Centro de Astrofísica Teórica, Universidad de los Andes, A. P. 26, La Hechicera, Mérida 5251, Venezuela
Email: lsigalot@cassini.ivic.ve
[2] Centro de Física, Instituto Venezolano de Investigaciones Científicas, IVIC, Apdo. 21827, Caracas 1020A, Venezuela
[3] Departamento de Física, FEC, Universidad del Zulia, Maracaibo, Venezuela